



# IJRASET

International Journal For Research in  
Applied Science and Engineering Technology



---

# INTERNATIONAL JOURNAL FOR RESEARCH

IN APPLIED SCIENCE & ENGINEERING TECHNOLOGY

---

**Volume: 6      Issue: IV      Month of publication: April 2018**

**DOI: <http://doi.org/10.22214/ijraset.2018.4469>**

**[www.ijraset.com](http://www.ijraset.com)**

**Call:  08813907089**

**E-mail ID: [ijraset@gmail.com](mailto:ijraset@gmail.com)**

# Wear Behaviour of Aluminium 7075 based Composites Reinforced with SiC, Red Mud and $Al_2O_3$

<sup>1</sup>Paras Mitta, Gianender<sup>2</sup>, Rinki Yadav<sup>3</sup>

<sup>1</sup>M.Tech. Scholar, Faculty of Mechanical Engineering Department, Manav Rachna University, Faridabad, Haryana-121004

<sup>2,3</sup>Faculty of Mechanical Engineering Department, Manav Rachna University, Faridabad, Haryana-121004

*The present research work on the abrasive wear behavior of aluminium metal matrix composite reinforcement with red mud, SiC, and  $Al_2O_3$  with an objective to explore the use of red mud, SiC and  $Al_2O_3$  as a reinforcing material due to its easy availability and the presence of all the reinforcing elements required. The microhardness studies and the wear performance were carried out by the variation in the percentage of reinforcements in the matrix. A Computerized pin-on-disc machine was used to assess the wear characteristics of the aluminium alloy 7075 with red mud, SiC and  $Al_2O_3$  Composites. To measure the value of microhardness number, microhardness tester was employed. The specimens were studied under optical microscope and SEM to know the distribution pattern of the reinforcement. The wear behaviour of the composite and the hardness of the matrix material are also improved due to the dispersion of particulates in the aluminium matrix.*

**Keywords:** Al7075, Red mud, Silicon Carbide (SiC), Stir Casting, Wear Behaviour, Scanning Electron Microscope (SCM), Microhardness

## I. INTRODUCTION

Aluminium is the most abundant and easily available metal in the Earth's crust after oxygen and silicon. It can be easily machined, drawn, cast and extruded. Its resistance to corrosion is also excellent due to a thin surface layer of Aluminium oxide that forms when the metal is exposed to air, preventing it from further oxidation. The typical aluminium alloying elements are Cu, Mg, Mn, Si, and Zn and are classified as cast alloys and wrought alloys. Wear is the progressive reduction of material from contacting surfaces in relative motion. The major concentration is imparted to study the wear behaviour, and hardness of aluminium based metal matrix composites AMC's which are generally used in agricultural, automotive and aerospace<sup>1,2,3</sup> industries because of its high strength to weight ratio<sup>4</sup>. Some aluminium components may have experienced faulty heat treatments before their installation in aircrafts<sup>5</sup>. Green<sup>6</sup> reviewed the techniques that do not require the removal of components which minimizes the aircraft down time and are non-destructive.

One of the important phenomena that take place at a material's interface is metal matrix composites with reinforcements that offer improved performance and wear resistance<sup>7</sup>. The metal matrix composites (MMC's), consists of at least two physically and chemically distinct phases, which may be either fibrous or particulate phase in a metallic matrix. The wear properties of the hybrid composites containing graphite exhibited the superior wear resistance properties<sup>8</sup>, which is in relevance to the present study. The most commonly used matrix materials are a copper matrix, aluminium matrix, and titanium matrix. The methods which are used to manufacture the particulate reinforced MMC's are solid fabrication methods, containing powder blending and consolidation and foil diffusion bonding; liquid phase fabrication methods, under which Electroplating/ electroforming, stir casting, squeeze casting, spray deposition, etc. are done. The main focus is on "stir casting" as this fabrication method is used to reinforce the material in the matrix. The reinforcement is fibers, particles/particulates, etc. embedded in the matrix (metals, polymers) is done in a composite material. This reinforcement is done at a microscopic level and is insoluble in each other. The most commonly used materials in the composite fabrication of Aluminium are 2000, 5000, 6000 and 7000 series alloys<sup>9</sup>. The reinforced materials which are used for Al7075 composite are Silicon carbide (SiC)<sup>10,11</sup>, Aluminium oxide ( $Al_2O_3$ ) and Graphite in the form of particles or whiskers<sup>12,13,14,15,16</sup>. There are certain factors like the wettability between the two main substances, Porosity in cast metal matrix composites, uniform distribution of the reinforcing material and the chemical reactions between the reinforcing material and the matrix alloy, which must be taken care of; so that the Dimensional stability, wear and corrosion resistance and reduction in weight are obtained in metal matrix composites. The effect of porosity on the wear and friction of metals and the surface roughness of the

materials, decrease in real contact area between two sliding surfaces were enhanced by pores<sup>17</sup>. Porosity decreases the wear resistance and coefficient of friction of the composite<sup>18</sup>. The microstructural analysis was performed using scanning electron microscopy, optical microscopy and image analysis<sup>19</sup>. For the fractographic study of engineering materials, scanning electron microscopy (SEM) is served to be the very useful technique. Dry sliding wear tests were conducted on a pin-on-disc machine<sup>20</sup>. For composite reinforcement, if the melt is combined with particulates, then ‘Stir casting’ is a very economical technique<sup>21</sup>. Stir casting is the conventional and economical way of producing AMCs<sup>22</sup> and these AMCs can be fabricated in many ways by its end uses. The set-up for stir casting is a furnace and stirring assembly. In the solidification synthesis of metal matrix composites, a melt of the selected matrix material which is followed by the introduction of a reinforcing material into the melt. Then the solidification of the melt under selected conditions is used to obtain the desired distribution of the dispersed phase in the matrix, containing suspended dispersoids. In friction stir processing (FSP), rotational tool speed is one of the most important process parameters which influence the uniform distribution of reinforcement particles, grain refinement, and heat input during the process<sup>23,24</sup>.

## II. PROBLEM FORMULATION

The study of wear behaviour of Al-red mud, SiC, Al<sub>2</sub>O<sub>3</sub> metal matrix composites (MMC’s) of aluminium alloy 7075 with varying percentage addition of red mud, SiC and Al<sub>2</sub>O<sub>3</sub> by the stir casting technique is the problem associated. By preparing the samples of different percentage composition by stir casting and then subjected them to the computerized pin on the disc wear testing machine, the experiments were performed. Then the analysis of microstructure was conducted by an optical microscope, scanning electron microscope and the dispersion of reinforcement was verified. On different types of specimens, the tests performed are the wear test performed on a computerized pin on disc M/C, micro hardness test on Vicker’s micro hardness tester, the microstructure test on the microscope and scanning electron microscope test performed on SEM.

## III. EXPERIMENTAL DETAILS

Machines/equipments used for performing the experiment and testing of composites are: weighing machine, digital control muffle furnace, radial drilling machine, micro hardness testing machine, SEM, sieve shaker, matrix (Al alloy 7075), reinforcements (red mud, SiC, Al<sub>2</sub>O<sub>3</sub>), Crucible, mould, stirrer, etc.

### A. Fabrication of Material

The chemical composition of Al 7075 matrix alloy and range of particle size of red mud, SiC and Al<sub>2</sub>O<sub>3</sub> are shown in table 1 and 2.

Table 1– Chemical Composition of Al 7075 Alloy

Al	Zn	Mg	Cu	Cr	Fe	Mn	Si
90 %	5.6 %	2.5 %	1.6 %	0.23 %	0.5 %	0.3 %	0.4 %

Table 2-Particle size range of Red Mud, SiC, and Al<sub>2</sub>O<sub>3</sub>

Reinforcement	Particle Size range (µm)
Red Mud	103-150
Silicon Carbide (SiC)	60-90
Alumina	30-50

‘Al’ MMC’s preparation by stir casting setup is shown in Figure 1. It consists of a resistance muffle furnace and a stirrer assembly. The stirrer assembly itself consisting of graphite stirrer, which is connected to a vertical drilling machine with a range of 80 to 890 rpm. The stirrer consists of 3-blades at an angle of 120 degrees apart. Inside the furnace, a clay graphite crucible of 1.5 kg capacity was placed and approximately 1kg alloy was melted at 820<sup>0</sup>C. In the resistance furnace, for one hour, reinforcement (red mud at 400<sup>0</sup>C, sic and alumina at 800<sup>0</sup>C) was preheated to remove the moisture and gases from the particular surfaces. Then the particles of reinforcement were sieved by sieve shaker shown in Figure 2.

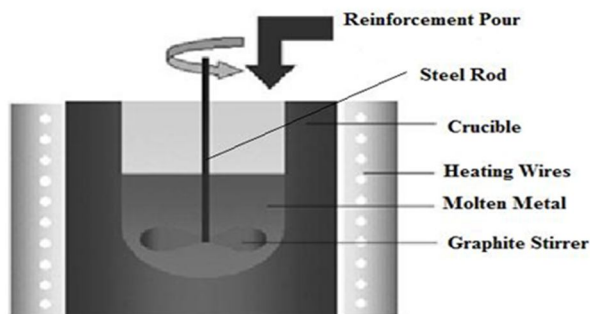


Fig. 1 – Graphical representation of Stir Casting

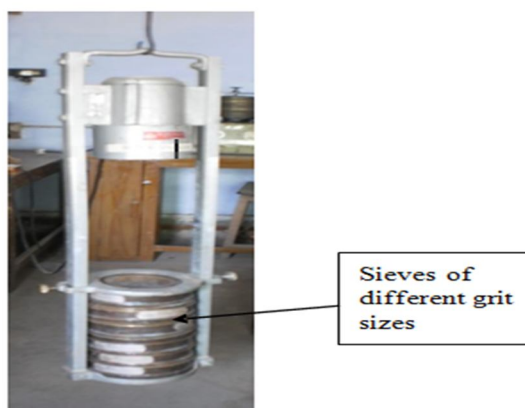


Fig. 2 – Sieve Shaker

The stirrer was then lowered vertically up to 3 cm, and its speed was gradually increased to 800 rpm, and the preheated reinforced particles were added at the rate of 10-20 g/min into the melt. As the stirrer speed got reduced by 50-60 rpm due to the increase in viscosity of the melt, the speed control maintained a constant speed of the stirrer, and then the stirring was continued for 8 to 12 minutes for proper mixing.

**B. Microhardness Test**

Micro hardness testing was done to measure the micro hardness; on a microscopic scale and was then calculated by using MVH-2 digital micro hardness tester, as shown in Figure 3. A precision diamond indenter is impressed into the materials at load from a few grams to 1 kilogram. The impression length measured microscopically, and the applied load are used to calculate a hardness value as shown in Figure 4. The indentations are typically made using either a square-based pyramid indenter (Vickers hardness scale) or an elongated, rhombo-hedral-shaped indenter. The tester applies the selected test load using dead weights. The length of the hardness impressions was precisely measured with a light microscope using either a flair eyepiece or a video image and computer software. A hardness number is then calculated using the test load, the impression length, and a shape factor for the indenter type used for the test.

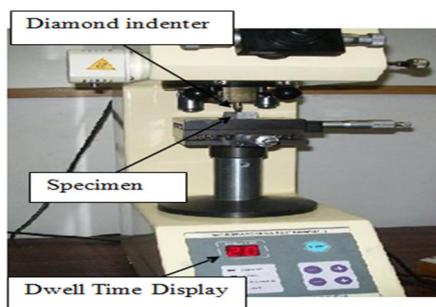


Fig. 3 – Vicker's Micro Hardness Tester





Fig. 4 – Micro indentation at 10X optical zoom

### C. Wear Test

Dry sliding wear tests for a different number of specimens was conducted by using a pin-on-disc machine (Model: Wear and Friction Monitor TR-20) supplied by DUCOM, was shown in Figure 5. The pin was held against the counter face of a rotating disc (EN32 steel disc) with wear track diameter 60mm. The pin was loaded against the disc through a dead weight loading system. The wear test for all specimens was conducted under the normal loads of 2kg and a fixed sliding velocity of 1.6 m/s. Wear tests were carried out for a total sliding distance of approximately 2900m. The pin samples were 50 mm in length and 8 mm in diameter. The surfaces of the pin samples were slides using emery paper (80 grit size) before the test in ordered to ensure effective contact of fresh and flat surface with the steel disc. The samples and wear track were cleaned with acetone and weighed (up to an accuracy of 0.0001 gm. using microbalance) before and after each test. The wear rate was calculated from the height loss technique and expressed regarding wear volume loss per unit sliding distance. Initially, pin surface was made flat such that it will support load over its entire cross-section called the First Stage. Run-in-wear was performed in the next stage / Second stage. This stage avoids initial turbulent period associated with friction and wears curves. Final stage / Third stage is the actual testing called constant/ steady state wear. This stage is the dynamic competition between material transfer processes (transfer of material from pin onto disc and formation of wear debris and their subsequent removal).

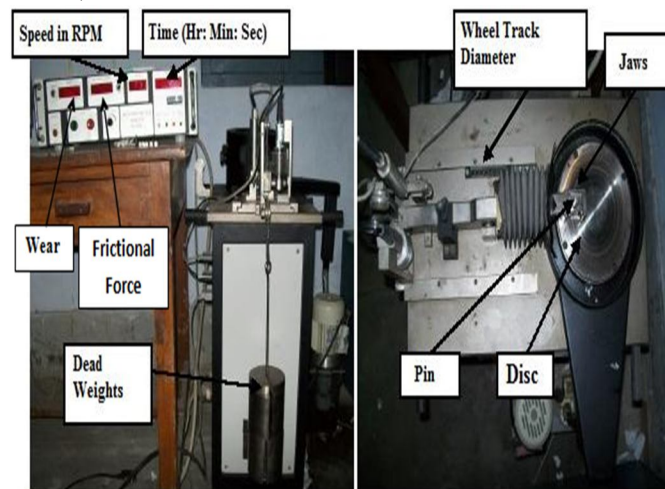


Fig. 5 – Wear Testing Machine

Table 3 – Experimental Parameters such as Load, Speed And Time

Load	2 Kg
Speed (V)	1.6 m/s
Total Time	30 min

Before starting the experiment, precautionary steps were taken to make sure that the load applied is in the normal direction. A schematic view of pin-on-disc setup is shown in Fig. 6.

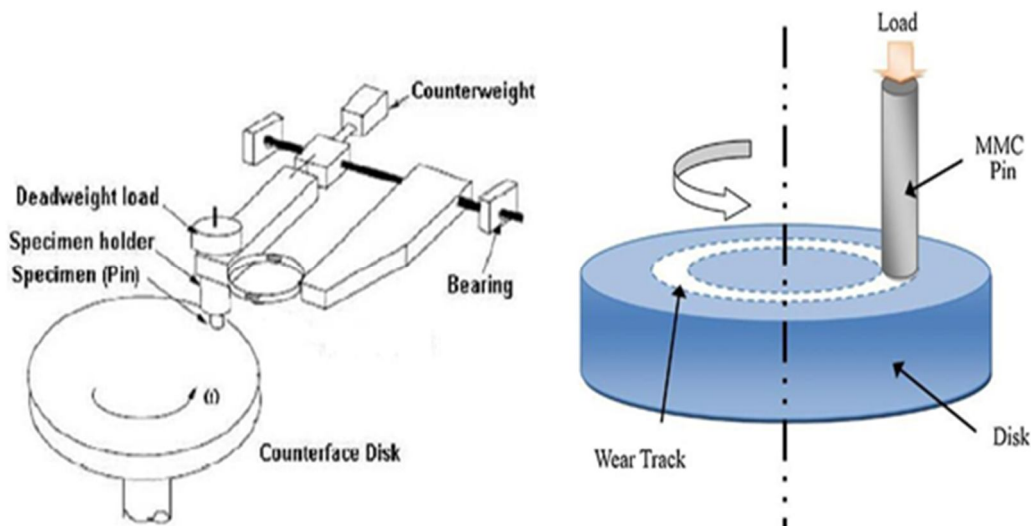


Fig. 6 – Pin on disc apparatus schematic

*D. Optical Microscopy*

Particles distribution was evaluated with the help of optical microscope. XRD studies were carried out to confirm the presence of reinforcement in the alloy matrix. The casting samples were examined under the optical microscope to determine the reinforcement pattern and cast structure. A section was cut from the castings. They were grinded using 100 grit silicon carbide paper followed by 220, 400, 600 and 1000 grades of emery paper. Before optical observation, the samples were mechanically polished and etched by Keller’s reagent to obtain better contrast.

**IV. RESULTS AND DISCUSSIONS**

*A. Micro Hardness Test*

For the measurement of micro hardness, a micro hardness tester MVH-1 is used on the Vicker’s micro hardness tester; load used was 200 grams at 10 X optical zoom with 20 second dwell time for each sample. The results obtained for alloy 7075 without reinforcement (Sample 1) and wt.% variation of different reinforcements in Al alloy 7075 MMC’s (sample no. 2-13) are shown in Table 4.

Table 4 – Micro Hardness value of samples

Sample No.	Sample Name (Al 7075)	Mean Micro Hardness
1	Pure (Base Alloy)	49.7461675
2	2.5 % SiC	57.30065
3	5% SiC	65.7694
4	7.5 % SiC	92.7731
5	10 % SiC	100.206025
6	2.5 % Al <sub>2</sub> O <sub>3</sub>	90.45515
7	5 % Al <sub>2</sub> O <sub>3</sub>	99.4015
8	7.5 % Al <sub>2</sub> O <sub>3</sub>	109.699925
9	10 % Al <sub>2</sub> O <sub>3</sub>	110.8675
10	2.5 % Red Mud	60.2283575
11	5 % Red Mud	76.6930125
12	7.5% Red Mud	114.2908
13	10% Red Mud	104.01875

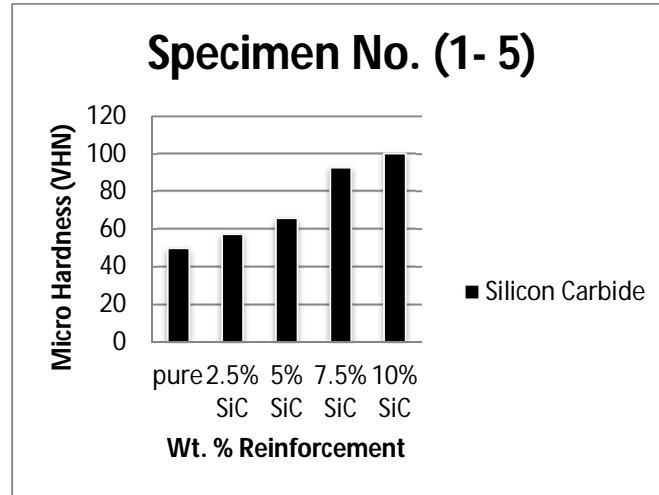


Fig. 7 – Comparison the Micro Hardness of alloy and MMCs with wt. % variation of SiC

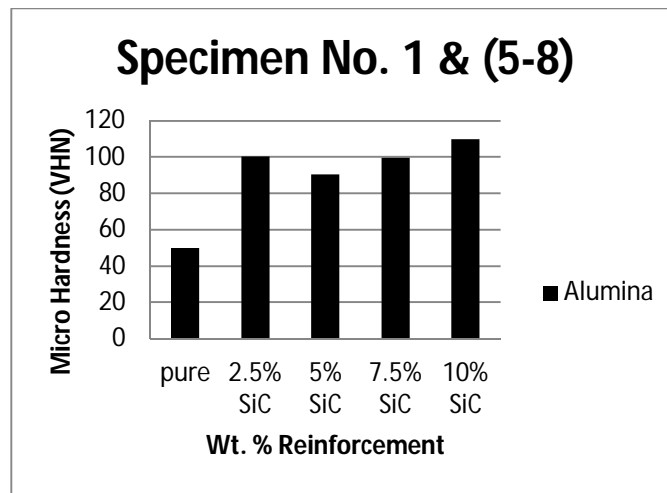


Fig. 8 – Comparison the Micro Hardness of alloy and MMCs with wt. % variation of Al<sub>2</sub>O<sub>3</sub>

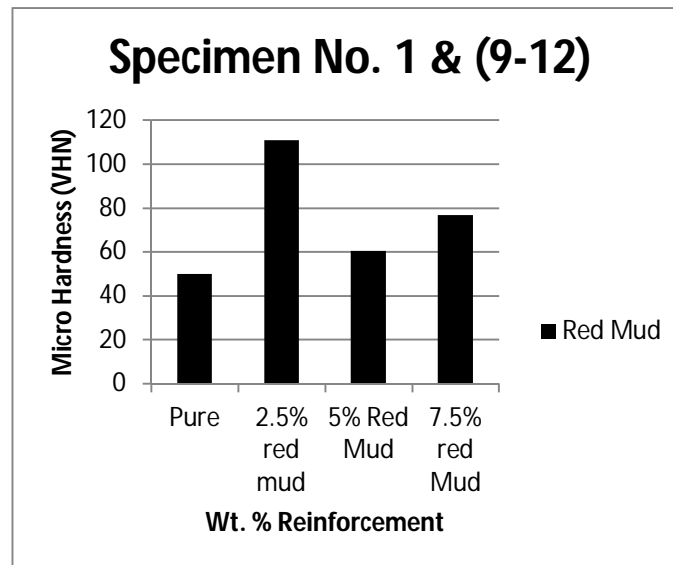


Fig. 9 – Comparison the Micro Hardness of alloy and MMCs with wt. % variation of Red Mud

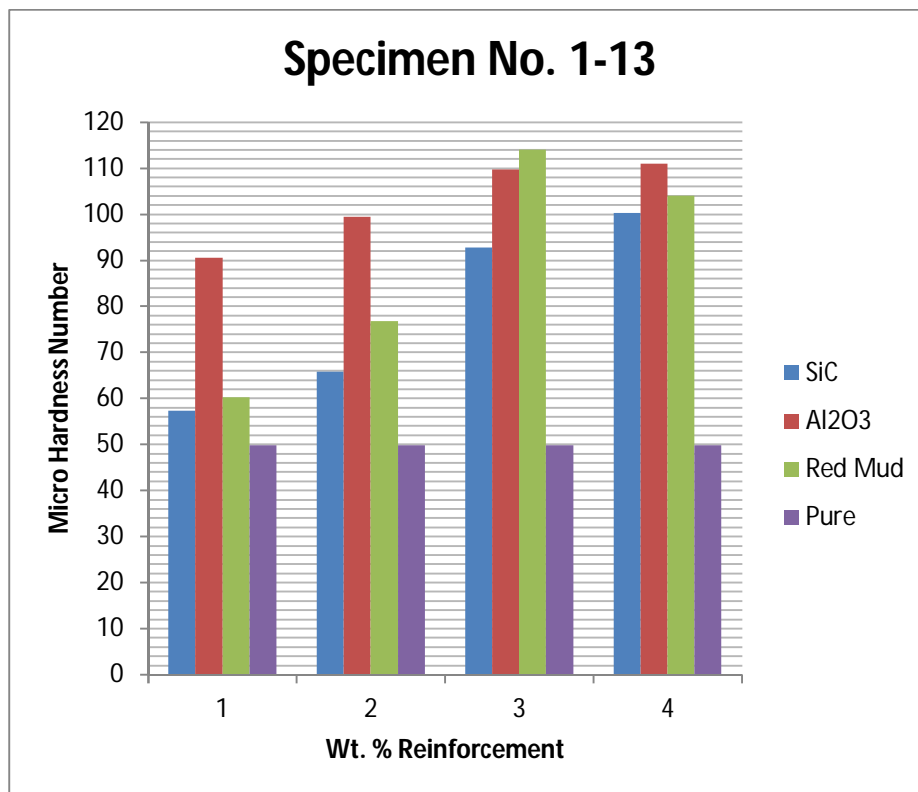


Fig.10 – Comparison the Micro hardness of alloy and all different MMCs

Figure 7 to Figure 10 shows the micro hardness of Al alloy and Al based MMCs reinforced with SiC, Al<sub>2</sub>O<sub>3</sub> and Red Mud. It is observed that hardness of alumina and Red Mud reinforced composite is more than that of SiC reinforced composite.

It can be attributed to the higher hardness of red mud and alumina compared to SiC particles. The hardness of alumina and red mud reinforced composite is more than that of SiC composite, attributes to the higher hardness of red mud and alumina compared to SiC particles. From the Figure 7 to Figure 8 shows that as the percentage of reinforcement increases, the micro hardness also increases. However, in the case of red mud reinforcement (Figure 9), the value of micro hardness increases upto 7.5 wt.%, then decreases, due to the improper mixing and high viscosity of molten composites or poor interfacial bonding between the particle–matrix interfaces. In Figure 10 showed the maximum value of micro hardness number is for sample 9 (Al alloy 7075+7.5% red mud) and the minimum value is for sample 1 (Al alloy 7075+2.5% SiC).

**B. Wear Test**

A pin-on-disc tribometer is used to perform the wear experiment, and the wear track, alloy, and composite specimens are cleaned with acetone, and then each specimen is weighed using a digital balance with an accuracy of ±0.0001 gm. The sliding speed 1.6 m/s, track dia. 60 mm, load 2 kg and total time 30 minutes are fixed for all experiments under room temperature as shown in table 5. Weight loss of MMC’s shown in Table 6.

Table 5 – Specifications of Wear Test

Length (mm)	Diameter (mm)	Velocity (m/s)	Track Dia (mm)	Weight (Kg)	Time (sec)
50	8	1.6	60	2	1800



Table 6 – Weight Loss of alloy and composites

Sample No.	Specimen Name	Initial Weight	Final Weight	Weight loss (gm.)
1	2.5 % SiC	6.7189	6.7033	0.0156
2	5% SiC	6.861	6.8466	0.0150
3	7.5 % SiC	6.6291	6.6182	0.0109
4	10 % SiC	6.3094	6.2988	0.0105
5	2.5 % Al <sub>2</sub> O <sub>3</sub>	5.8463	5.8211	0.0252
6	5 % Al <sub>2</sub> O <sub>3</sub>	6.1684	6.1506	0.0177
7	7.5 % Al <sub>2</sub> O <sub>3</sub>	5.5094	5.4929	0.0165
8	10 % Al <sub>2</sub> O <sub>3</sub>	5.8910	5.8768	0.0141
9	2.5 % Red Mud	6.1592	6.1337	0.0255
10	5 % Red Mud	5.8250	5.8011	0.0239
11	7.5% Red Mud	6.1720	6.1524	0.0196
12	10% Red Mud	5.7105	5.6872	0.02322
13	Base alloy	60646	6.6208	0.0254

The results predicted that as the wt.% of reinforcement increases, weight loss of MMC's decreases. However, the weight loss decreases up to 7.5 wt.% and then increases in case of red mud. It is also clear that the maximum weight loss is for sample 9 (Al alloy 7075+2.5% red mud) and minimum weight loss for sample 4 (Al alloy 7075 +10% SiC) occurs. Comparing the weight loss properties of composites reinforced with silicon carbide, alumina, and red mud, it is observed that despite their higher hardness, composites reinforced with alumina and red mud particles show greater weight loss as compared to composites reinforced with SiC particles.

Table 7 – Wear loss of MMC's and alloy v/s Time

Wear loss (µm) vs time (sec)	300	600	900	1200	1500	1800
Sample 1 (alloy + 2.5% SiC)	75.75	107.21	136.7	166.24	195.92	222.73
Sample 2 (alloy + 5% SiC)	67.85	96.79	113.55	130.8	146.75	167.59
Sample 3 (alloy + 7.5% SiC)	42.58	64.08	87.22	106.8	125.13	145.31
Sample 4 (alloy + 10% SiC)	38.31	57.99	78.86	101.57	120.56	140.38
Sample 5 (alloy + 2.5% Al <sub>2</sub> O <sub>3</sub> )	106.38	140.48	170.43	201.33	229.99	257.79
Sample 6 (alloy + 5% Al <sub>2</sub> O <sub>3</sub> )	102.75	144.87	171.64	193.91	224.99	262.86
Sample 7 (alloy + 7.5% Al <sub>2</sub> O <sub>3</sub> )	78.48	124.67	159.76	199.03	228.99	255.7
Sample 8 (alloy + 10% Al <sub>2</sub> O <sub>3</sub> )	66.91	100.93	131.48	163.01	193.39	218.24
Sample 9 (alloy + 2.5% RM)	64.88	132.98	189.86	235.48	281.78	308.55
Sample 10 (alloy + 5% RM)	138.55	163.41	189.14	215.17	243.84	270.19
Sample 11 (alloy + 7.5% RM)	44.24	78.68	124.76	174.44	217.43	269
Sample 12 (alloy + 10% RM)	88.2	129.77	174.54	227.77	266.96	302.99
Sample 13 (alloy)	68.98	142.66	192.01	232.02	268.04	302.2

Sliding wear loss and wear rate performance of different specimens with and without reinforcement into the matrix (1-13) under a dry sliding condition at ambient temperature were found using a pin-on-disc apparatus and the wear loss of the MMC's of sample number 1-13 for aluminium and composites is shown in Table 7.

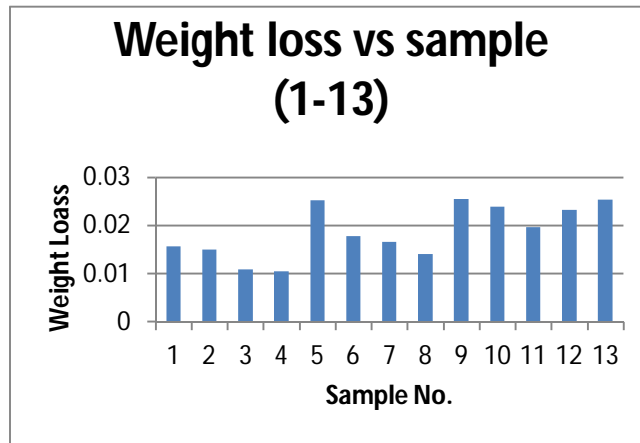


Fig. 11 – Weight Loss of alloy and composites

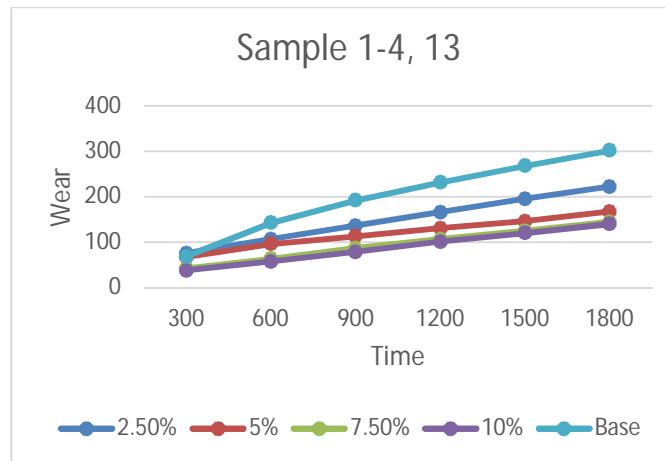


Fig. 12 - Wear in Micrometers Vs. Time in seconds of Samples (1-4, 13)

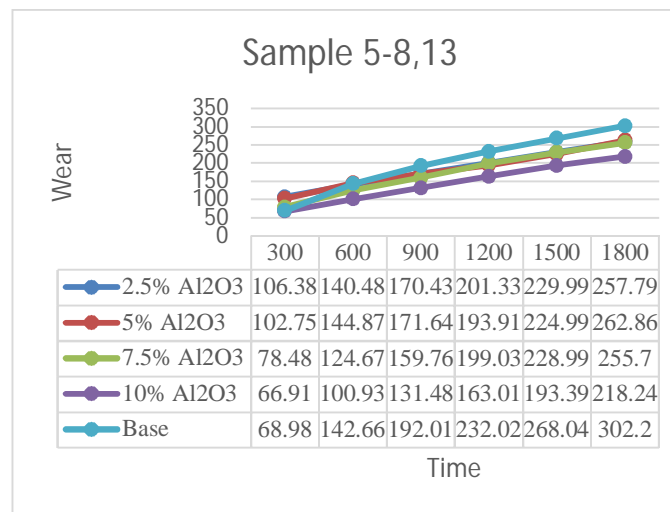


Fig. 13 - Wear in Micrometers Vs Time in seconds of Samples (5-8, 13)

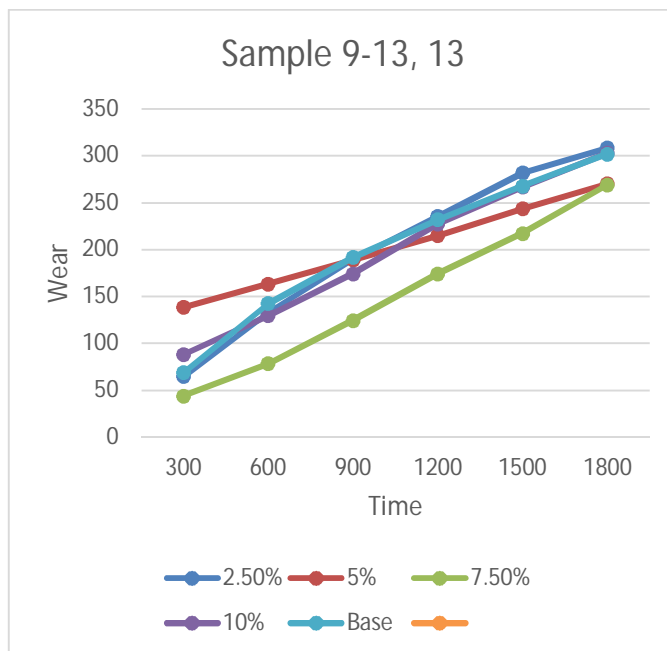


Fig. 14 - Wear in Micrometers Vs Time in seconds of Samples (9-13, 13)

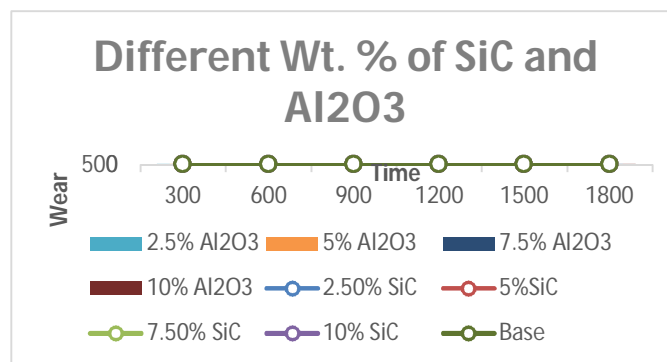


Fig. 15 - Wear in Micrometers vs. time in seconds

The Figure shows the wear loss as a function of time for the Al alloy 7075 and composites reinforced with silicon carbide, alumina and red mud particles of different size ranges (60- 90  $\mu\text{m}$ , 30-50  $\mu\text{m}$  and 103-150  $\mu\text{m}$ ) at a constant load of 20 N and total time is 30 minutes. The results revealed that the wear loss of Al alloy 7075 decreases after addition of Al<sub>2</sub>O<sub>3</sub>, SiC, and particles of red mud. It attributes to the increase in hardness of the material due to the presence of hard ceramic particles. Comparing the wear properties of composites reinforced with silicon carbide, alumina, and red mud, it is observed that despite their higher hardness, composites reinforced with alumina and red mud particles show poor wear resistance as compared to composites reinforced with SiC particles. It can be attributed to the comparatively poor bonding between the red mud-matrix and in alumina-matrix. There might be particle pull out, in the case of composite reinforced alumina and red mud particles during wear test, which enhances wear loss. Figure 12 to Figure 14 shows the variation of wear loss with time (total time is taken to be 30 min) for constant load 2 Kg at 510 rpm. It can be observed from the plots that with the addition of SiC, Al<sub>2</sub>O<sub>3</sub> and Red Mud Particulates in the matrix the wear loss of composites was decreased. Also as the time increases the wear loss increases.

The results as indicated from Figure 12 the decreasing trend of wear loss with an increase in weight percentage of SiC up to 10% weight fraction. Similarly, the results as indicated from Figure 13 the decreasing trend of wear loss with an increase in weight percentage of Al<sub>2</sub>O<sub>3</sub> up to 10% weight fraction. From the comparison graph Fig. 15, i.e., different wt. % of SiC Vs. Al<sub>2</sub>O<sub>3</sub> shows that 10% SiC has the superior wear resistance property over the other different wt. % of reinforcements in the case of wear loss. Similarly, 10% SiC has superior wear resistance property over the other different wt.% of reinforcements in the case of wear loss.

Wear rate and wear resistance for MMC's can be obtained by using this formula:

**Wear Rate:** It is defined as wear volume per unit distance travelled.

$$\text{Wear Rate} = \text{Wear Volume (mm}^3\text{)} / \text{Sliding distance (m)}$$

Sliding distance can be calculated as:

$$\text{Sliding distance} = \text{Sliding Speed} * \text{Time} = (\pi D N / 60) t$$

$$\text{Wear Volume} = \pi r^2 h$$

where, D = Diameter of wheel track (60mm),

r = radius of pin (4 mm),

h = cumulative wear height loss (mm),

N = R.P.M (510)

t = Time duration in seconds

V = Sliding Speed (1.6 m/s).

( $\pi$  = 3.14 (constant))

**Wear Resistance:** Wear resistance is a reciprocal of wear rate. Wear resistance = 1 / wear rate

Wear rate of MMC's (sample no.1-12), and alloy (sample 13) is shown in table 8. It is observed that wear rate decreases with increase in wt.% of SiC and Al<sub>2</sub>O<sub>3</sub> while in the case of red mud, it firstly decreases up to 7.5 % wt. Addition and after 7.5 wt. Increases due to the increased viscosity and improper rotation of stirrer. Wear resistance of the composites is improved by the depression of SiC, red mud and Al<sub>2</sub>O<sub>3</sub> particles.

Table 8 - Wear rate of MMCs and alloy Vs. Sliding Distance

C. Microstructure Test

Sliding Distance (m)	500	1000	1500	2000	2500	3000
Wear Rate X10 <sup>-3</sup> (mm <sup>3</sup> /m)						
Sample 1 (alloy + 2.5% SiC)	7.7742	5.5025	4.755	4.292	4.0716	3.9014
Sample 2 (alloy + 5% SiC)	6.9822	4.9230	3.9333	3.3814	3.0046	2.9210
Sample 3 (alloy + 7.5% SiC)	4.45	3.391	2.919	2.7913	2.6250	2.5378
Sample 4 (alloy + 10% SiC)	4.0741	3.0055	2.6963	2.6528	2.5345	2.4532
Sample 5 (alloy + 2.5% Al <sub>2</sub> O <sub>3</sub> )	10.7155	7.1947	5.8094	5.1872	4.7109	4.5122
Sample 6 (alloy + 5% Al <sub>2</sub> O <sub>3</sub> )	10.4351	7.3611	5.9394	5.0725	4.6791	4.5912
Sample 7 (alloy + 7.5% Al <sub>2</sub> O <sub>3</sub> )	8.1214	6.4943	5.5803	5.181	4.7187	4.4628
Sample 8 (alloy + 10% Al <sub>2</sub> O <sub>3</sub> )	7.0314	5.2639	4.5571	4.2382	3.9646	3.8340
Sample 9 (alloy + 2.5% RM)	13.5954	8.0395	6.6942	6.0082	5.5602	5.6087
Sample 10 (alloy + 5% RM)	14.0122	8.3382	6.4671	5.5008	5.0136	4.7181
Sample 11 (alloy + 7.5% RM)	5.444	4.6935	4.5838	4.473	4.2424	4.1593
Sample 12 (alloy + 10% RM)	7.8969	7.4129	6.625	6.2136	5.6657	5.4069
Sample 13 (alloy)	15.2882	8.7967	6.3692	5.0981	4.8193	4.7103

1) *Optical Microscope*: The microstructure was visualized with the help of an optical microscope. The specimens were visualized on 100X magnifications to show the presence of reinforcement and its distribution in the metal matrix. Different elements/compounds which were present in the red mud are difficult to distinguish by optical microscopy. The microstructure of all the samples was shown in Figure 16.

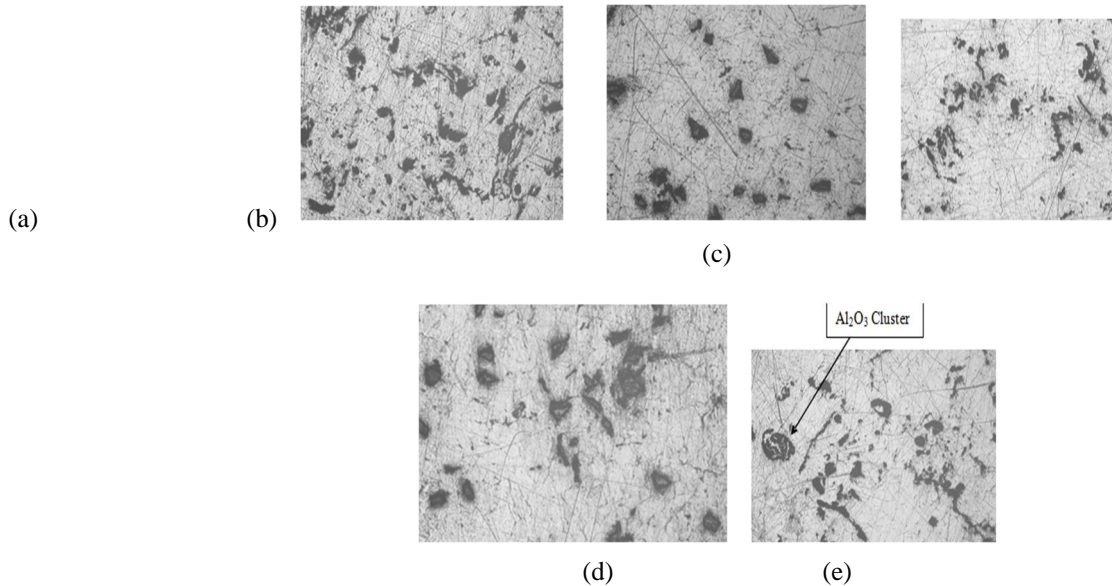


Fig. 16 - Optical micrographs of Al alloy (100X) (a) 7075 (b) with 2.5 wt. %  $Al_2O_3$  (c) with 5 wt. %  $Al_2O_3$  (d) with 7.5 wt. %  $Al_2O_3$  (e) with 10 wt. %  $Al_2O_3$ .

It is clear from the Figure 16 that the distribution of  $Al_2O_3$  particles in a matrix alloy is fairly uniform. The average size of  $Al_2O_3$  particles is around  $30\mu m$ - $50\mu m$ . The shape of most  $Al_2O_3$  particles is irregular in nature. The irregular shape of aluminium oxide particles may be due to the breakage of particles during ball milling. It is found that as the percentage of reinforcement increases the area fraction also increases as shown in the optical micrograph. It also observed that there is an increase in hardness and wear resistance this can be attributed to the increase in the interfacial bonding of reinforcement with the aluminium matrix alloy. Good interfacial bonding can be obtained by pre-heating of  $Al_2O_3$  particulates before adding in the matrix. It is also found that at some places there was clustering of  $Al_2O_3$  particulates as shown in Figure 15.

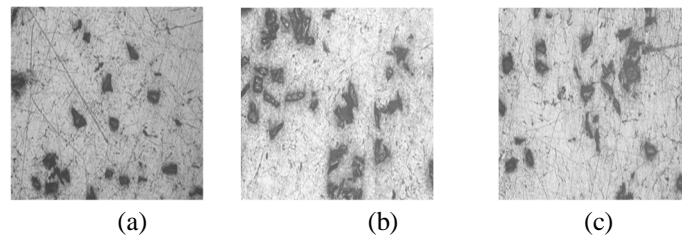


Fig. 17 - Optical micrographs of MMC with SiC (100X) (a) 2.5 wt.% (b) 5 wt.% (c) 7 wt.%

It is clear from the Figure 17 that the distribution of SiC particles in a matrix alloy is nearly uniform. The average size of SiC particles is around  $60\mu m$ -  $90\mu m$ . The shape of most SiC particles is angular and sub-angular. It is found that as the percentage of reinforcement increase the area fraction also increases as shown in the optical micrograph. It also observed that there is an increase in hardness and wear resistance this can be attributed to the increase in the interfacial bonding of reinforcement with the aluminium matrix alloy. Good interfacial bonding can be obtained by pre-heating of SiC particulates before adding in the matrix.

2) *Microstructural Observation of worn pin surfaces*: The worn-out surfaces of some selected/ typical specimens (10 % wt. a fraction of reinforcements) after the wear test were observed under an optical microscope with magnification 200X.



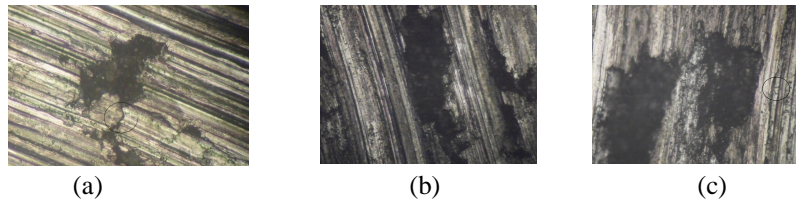
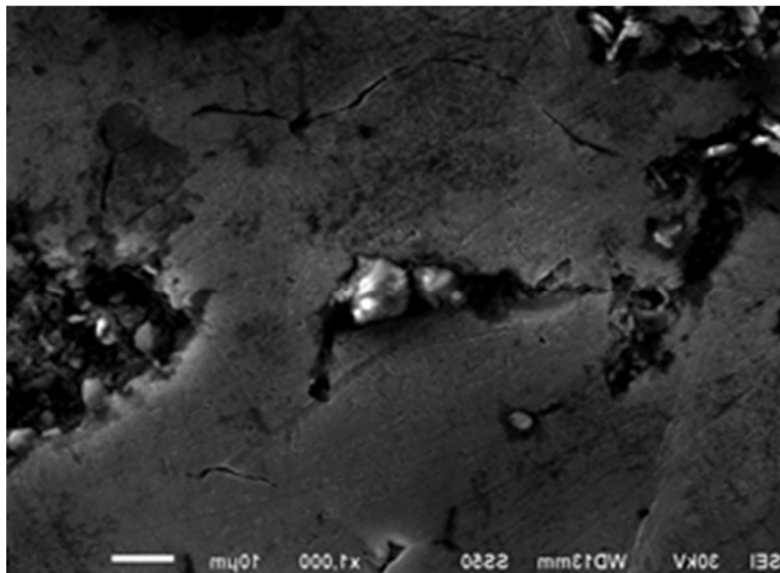


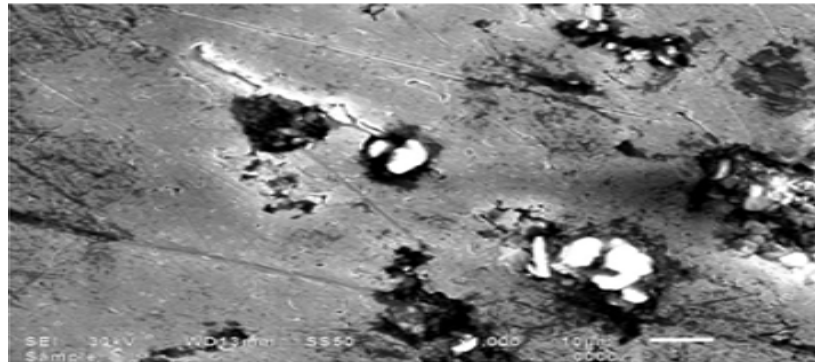
Fig. 18 - Micrograph showing wear surface of (a) 10% Red Mud in Al alloy 7075 (b) 10% SiC in Al alloy 7075 (c) 10% Al<sub>2</sub>O<sub>3</sub> in Al alloy 7075

Figure 18 shows the surface morphology of aluminium alloy 7075 with 10% Red Mud, SiC, and Al<sub>2</sub>O<sub>3</sub> composite, tested under ambient temperature with constant load and speed. The structures of the worn surfaces are greatly dependent on sliding speed, load, and hardness of particles (reinforcement). Comparing these Figures, it can be visualized that one of the common features observed in all three MMCs, i.e., the formation of grooves and ridges running parallel to the sliding direction. These wear scars are the primarily characteristic of abrasive wear. On further analyzing, it has been found that grooves are fine on the worn pin surface of Al alloy 7075 with 10 % wt. The fraction of SiC as compared to others. A similar observation was also reported in Al-Si alloy subjected to 24.5 N load in comparison to 53.9 N. From the micrographs [Figure 18 (a),(c)] some cracks have appeared, and these cracks are propagated in different directions. This might be due to strain hardening of aluminium based metal matrix composites with applied load and due to pulling up of hard phase particles, i.e., red mud and alumina from the aluminium grain boundary.

3) *Scanning Electron Microscopy Analysis:* Scanning electron micrographs at lower magnification show that the distribution of SiC, Al<sub>2</sub>O<sub>3</sub> and Red Mud particulate throughout the MMCs. Scanning electron micrographs at higher magnification show the particle–matrix interfaces. Homogeneous distribution of particles is desired for achieving better wear behaviour and mechanical properties. Homogeneous distribution of particles in a molten alloy is achieved due to the high shear rate caused by stirring which also minimize the particles settling. However, agglomeration of particles in some regions is visible in all cases; this is due to the presence of porosity associated with it. The presence of entrapped air and moisture in the reinforcement particles results in the voids/ porosity after casting. It is observed that the particle–matrix interface of Al<sub>2</sub>O<sub>3</sub> and Red Mud reinforced composite is not as smooth as that of SiC reinforced composite, which indicates relatively poor bonding between the alumina-Al alloy 7075 alloy matrix and Red Mud-Al alloy 7075 alloy matrix. At higher magnification, SEM shows the shape of most Red Mud particles exhibits globular morphology. Other different types of particle are also visible in red mud MMCs, but still, it is not possible to distinguish these different particles types. Further, the SEM reveals an excellent bond between the matrix alloy and SiC reinforcement particles.



(a)



(b)

Fig. 19 - SEM of MMC at 1000X (a) with 7.5 wt. % Al<sub>2</sub>O<sub>3</sub> (b) 10 wt. % Al<sub>2</sub>O<sub>3</sub>

## V. CONCLUSION

The significant conclusions of the studies carried out on Al7075 based composite reinforced with red mud, Al<sub>2</sub>O<sub>3</sub> and SiC MMCs are as follows:

- 1) Metal matrix composites of 'Al' are easily fabricated by the stir casting technique with a uniform distribution of red mud, SiC, and Al<sub>2</sub>O<sub>3</sub> particulates.
- 2) Stirrer design and position, stirring speed and time, particles incorporation rate and preheating temperature are the important parameters for the synthesis of stir casting process.
- 3) It is confirmed from the results that stir formed Al alloy 7075 with reinforced composites is superior to base Al alloy 7075 in comparison of microhardness.
- 4) Wear resistance of the composites is improved by the depression of SiC, red mud and Al<sub>2</sub>O<sub>3</sub> particles.
- 5) SiC, red mud and alumina addition is beneficial in the reduction of wear rate of composites.
- 6) Two stages of wear rate are shown for all applied loads that are run in wear upto 1 km sliding distance and wear rate approaches to steady state.
- 7) Wear rate decreases with increase in wt.% of SiC and Al<sub>2</sub>O<sub>3</sub> while in the case of red mud, it firstly decreases upto 7.5 % wt. Addition and after 7.5% wt. Increases due to the increased viscosity and improper rotation of stirrer.
- 8) The particulates of SiC, red mud and alumina are fairly distributed in the matrix, as revealed by optical micrography and SEM images, which also showed that at some places voids have occurred before wearing. The
- 9) groves, ridges, and cracks after wearing are obtained by optical micrography.

## VI. ACKNOWLEDGEMENTS

The authors would like to be obliged to Manav Rachna University, Faridabad for providing financial assistance for experimental work of the work.

## REFERENCES

- [1] Terry B. and Jones G., Metal Matrix Composites: Current Developments and Future Trends in Industrial Research and Applications, Elsevier Advanced Technology, Oxford, UK, 1990, 105.
- [2] Charles D., Metal matrix composites- ready for take-off, Metals Mater., 6 (1990) 78-82.
- [3] Zedalis M.S., Bryant J.D., Gilman P.S. and Das S.K., High-temperature discontinuously reinforced aluminium. J. Met., 43 (1991) 29-31.
- [4] Woei-Shyan Lee, Wu-Chung Sue, Chi-Feng Lin and Chin-Jyi Wu, The strain rate and temperature dependence of the dynamic impact properties of 7075 aluminium alloy, Journal of Materials Processing Technology, 100 (2000) 116-122.
- [5] R. Clark Jr, B. Coughran, I. Traina, A. Hernandez, T. Scheck, C. Etuk, J. Peters, E.W. Lee, J. Ogren and O.S. Es-Said, On the correlation of mechanical and physical properties of 7075-T6 Al alloy, Engineering Failure Analysis, 12 (2005) 520-526.
- [6] Green RE. Emerging techniques of NDE of aging aircraft structures, Materials research society symposia proceedings, Pittsburgh, PA: Materials Research Society, 503 (1998) 3-14.
- [7] Yilmaz O and Buytoz S., Abrasive wear of Al<sub>2</sub>O<sub>3</sub>- reinforced aluminium-based MMCs, Compos Sci Technol., 61 (2001) 2381-92.
- [8] A. Baradeswaran and A. Elaya Perumal, Wear and Mechanical characteristics of Al 7075/graphite composites, Compos. Part B Eng., 56 (2014) 464-471.
- [9] Deuis R. L., Subramanianm C. and Yellup, Dry Sliding Wear of Aluminium Composites – A Review, Composites Science, and Technology, 57 (1997) 415-435.
- [10] Alpas A. T. and Zhang J., Effect of Microstructure (Particulate Size and Volume Fraction) and Counterface Material on the Sliding Wear Resistance of Particulate-Reinforced Aluminum Matrix Composites, Metall. Mater. Trans., 25A (1994) 969-983.



- [11] Roy M., Venkataraman B., Bhanuprasad V.V., Mahajan Y.R. and Sundaraian G., The effect of particulate Reinforcement on the sliding wear behaviour of aluminium matrix composites, *Metall. Trans. A*, 23 (1992) 2833-2847.
- [12] Hassan AM, Alrashdan A, Hayajneh MT and Mayyas AT, Wear behavior of Al-Mg-Cu-based composites containing SiC particles, *Tribol Int*, 42 (2009) 1230-8.
- [13] Gui M and Kang SB, Dry sliding wear behavior of plasmasprayed aluminium hybrid composite coatings, *Metall Mater Trans A*, 32A (2001) 2383-92.
- [14] Tang F, Wu X, Ge S, Ye J, Zhu H, Hagiwara M and Schoenung JM, Dry sliding friction and wear properties of B4C particulate-reinforced Al-5083 matrix composites, *Wear*, 264 (2008) 555-61.
- [15] Zhan Y and Zhang G, Graphite and SiC hybrid particles reinforced copper composite and its tribological characteristic, *J Mater Sci Lett*, 22 (2003)1087-89.
- [16] Leng J, Jiang L, Wu G, Tian S, Chen G, Effect of graphite particle reinforcement on dry sliding wear of SiC/Gr/Al composites, *Rare Met Mater Eng*, 38 (2009)1894-8.
- [17] Vardavoulis M., Jouannt-Tresy C. and Jeandin M., Sliding wear behaviour of ceramic particle reinforced high-speed steel obtained by powder metallurgy, *Wear*, 165 (1993) 141-149.
- [18] Hamid Abdulhaqq A., Ghosh P.K., Jain S.C. and Ray S., Influence of particle content and porosity on the wear behavior of cast in situ Al(Mn)-Al<sub>2</sub>O<sub>3</sub>(MnO<sub>2</sub>) composite, *Wear*, 260 (2006) 368-378.
- [19] Zhang J., Perez R.J. and Lavernia E.J., Effect of SiC and graphite particulates on the damping behavior of metal matrix composites, *Acta Metallurgica et Materialia*, 42 (1994) 395-409.
- [20] Basavarajappa S., Chandramohan G., Mahadevan Arjun, Thangavelu Mukundan, Subramanian R. and Gopalakrishnan P., Influence of sliding speed on the dry sliding wear behavior and the subsurface deformation on hybrid metal matrix composite, *Wear*, 262 (2007) 1007-12.
- [21] Clyne, T.W., *Metal Matrix Composites: Matrices and Processing*. In: Mortensen, A., Ed., *Encyclopedia of Materials: Science and Technology*, Composites: MMC, CMC, PMC, Elsevier, New York, (2001) 1-14.
- [22] Gopalakrishnan S., Murugan N., Production and wear characterization of AA 6061 matrix titanium carbide particulate reinforced composite by enhanced stir casting method, *Composites: Part B Engineering*, 43 (2012) 302-308.
- [23] Azizieh M, Kokabi A H and Abachi P, Effect of rotational speed and probe profile on microstructure and hardness of AZ31/Al<sub>2</sub>O<sub>3</sub> nanocomposites fabricated by friction stir processing, *Mater. Des.*, 32 (2011) 2034–2041
- [24] Asadi P., Faraji G. and Besharati M.K., Producing of the AZ91/SiC composite by friction stir processing (FSP), *The Int. Journal of Advanced Manufacturing Technology*, 51 (2010) 247-60.





10.22214/IJRASET



45.98



IMPACT FACTOR:  
7.129



IMPACT FACTOR:  
7.429



# INTERNATIONAL JOURNAL FOR RESEARCH

IN APPLIED SCIENCE & ENGINEERING TECHNOLOGY

Call : 08813907089  (24\*7 Support on Whatsapp)